Characterization and Corrosion Behavior of Hydroxyapatite and Hydroxyapatite/ Titania Bond Coating on 316L SS Substrate in Simulated Body Fluid

Tejpreet Singh[1], Niraj Bala[1] and Lakhvir Singh[2]
[1,2]Mechanical Engineering Department, BBSBEC, Fatehgarh Sahib, Punjab, India
E-mail: [1]bedi06ts@gmail.com

Abstract—*The main aim of this study is to evaluate in-vitro corrosion behavior of thermal sprayed hydroxyapatite (HAp) and hydroxyapatite/ titania bond (HAp/TiO_2) coated 316L SS. The improved corrosion resistance is desired for many clinical applications and has become an emerging technology in biomaterials research and industry. The coatings were characterized by XRD, SEM techniques. The micro-structural morphology phases and electrochemical properties of the coatings were investigated. The corrosion behavior of the bare and coated specimens was carried out in simulated body fluid. The experiments were conducted for open circuit potential and potentio-dynamic polarization. The study showed that the HAp coated 316L SS specimens appeared more corrosion resistant than the uncoated and HAp/TiO_2 bond coated 316L SS specimens.*

Keywords: *HAp coatings, in-vitro, corrosion, biocompatibility*

Introduction

Biomaterials are used in vast range of biomedical applications such as surgical implants including joints, limbs, total hips, knees, artificial arteries, skins, dentures, heart valves, intra uterine devices, pacemaker leads and cardiovascular nets [1]. Metallic biomaterials have the longest history among the various biomaterials [2]. Stainless steels, Ti and its alloys and Co-Cr alloys are commonly employed as orthopedic implants because of their high strength compared to polymers and high toughness compared to ceramic materials [3]. The corrosion resistance of hydroxyapatite [$(Ca_{10}(PO_4)_6(OH)_2$), HAp] coatings on various metallic substrates in different physiological solutions has been investigated by many researchers [4-8]. Kwok *et al.* [4] reported that HAp coated Ti-6Al-4V possessed higher corrosion resistance compared to bare Ti-6Al-4V substrate in Hank's physiological solution due to lower corrosion current density and noble shift of open circuit potential [4]. Corrosion resistance of Ni-Ti alloy in simulated body fluid was improved by almost 60 times by electro-deposition of HAp-zirconia composite coating [5]. Bai *et al.* [6] deposited CNT-HAp coatings on titanium substrate and found better protection efficiency and good biocompatibility in simulated body fluid [6]. Gopi and co-workers deposited HAp coatings on borate passivated 316L SS and studied corrosion behavior of coatings in Ringer's solution. They reported polarization potential values of HAp coated 316L SS to be nobler than bare AISI 316L SS specimens [7]. HAp coated magnesium metal specimens were treated with 50 mol/m^3 Ca-EDTA/50 mol/m^3 KH_2PO_4 solution for 8, 16 and 24 hrs and were subsequently tested for corrosion resistance in 3.5 wt% NaCl solution by Hiromoto and Yamamoto [8]. They reported that HAp coated magnesium specimens were 1000 times lesser anodic current density compared to bare magnesium [8].

In the present study, HAp and HAp/TiO_2 powders were deposited on 316L SS specimens using a flame spraying technique. The micro-structural morphology phases and electrochemical properties of the coating were investigated. The corrosion testing of the bare and coated specimens was carried out in a simulated body fluid. The experiments were conducted for open circuit potential and potentio-dynamic polarization.

Experimental Procedure

Feedstock Powder and Substrate

The Captal 30, HAp powder (Plasma-Biotal, Tideswell, UK) of 30μm average particle size and Amperit 782.0, TiO_2 powder (H.C. Starck, Goslar, Germany) with a particle size distribution from 5–22 μm were used in this study. Commercially available stainless steel 316L SS with chemical composition (% wt): C-0.024Cr-16.850, Ni-10.735, Mo-2.269, Si-0.468, Mn-1.156, P-0.032, S-0.017, Fe-balance was used as the substrate. 316L SS coupons each measuring 15mm x 10mm x 2mm were prepared. The specimens were polished by silicon carbide papers down to 180 grit. The substrates were then grit blasted using grit blasting equipment. Al_2O_3 grits of 20 mesh sizes were used during the grit blasting operation at a pressure of 5 bars for 2 minutes. The substrates were subsequently air blasted to remove any residual grit.

Development of Coatings

The air blasted 316L SS specimens were coated with the HAp and HAp/TiO_2 powders using CERAJET flame spraying apparatus available at Metallizing Equipment Company Private Limited (MECPL) Jodhpur, India. CERAJET is proprietary product of MECPL especially designed for ceramic coatings. The specimens were

coated up to a coating thickness of 150–170 μm using CERAJET flame spraying system. The particle velocity of conventional flame spraying systems was less than 100m/s whereas the particle velocity of a present flame spraying system was ≈300m/s. The temperature of the oxyacetylene flames in CERAJET system was ≈2700°C which is much lower than the plasma spraying technique. The spraying parameters used for HAp and HAp/TiO_2 coatings are shown in Table1 given below:

Table 1: Flame Spray Process Parameters for HAp and HAp/ TiO_2 Coatings

Acetylene Flow Rate	73 L/min
Oxygen Flow Rate	44 L/min
Air Pressure	4.5 kgf/cm^2
Powder Feed Rate	15 g/min
Spray Distance	10 cm

The phase composition of the as-sprayed coatings was analyzed by an XRD machine (X'pert-PRO) with Cu Kα radiation operating at 40 kV/30 mA. The coated samples were scanned over the 2θ range of 20-60˚. The micro-structural characterization and morphology of as-sprayed specimens was examined by JSM-6610 (JEOL Scanning Electron Microscope) coupled with EDS. SEM analysis of the coated samples was done to study their surface morphology. EDS analysis was performed in order to evaluate Ca/P ratios of the HAp and HAp/TiO_2 coatings. All specimens were cleaned to degrease in acetone before they were immersed in the experimental solution for electrochemical polarization.

Electrochemical Corrosion Studies

To investigate the electrochemical corrosion behavior of the bare, HAp coated and HAp/TiO_2 bond coated 316L SS specimens, the potentiodynamic polarization tests were conducted using a Potentiostat/Galvanostat (Series G-750 Gamry Instruments, Inc. USA) interfaced with a computer and loaded with Gamry electrochemical software DC105. The electrolyte used for simulating human body fluid conditions was Ringer's solution with chemical composition as NaCl-8.90g/L, $CaCl_2$-0.24g/L, KCl-0.43g/L and $NaHCO_3$-0.2g/L at pH-7.2. Before conducting the corrosion studies, each specimen was immersed in Ringer's solution for 24 hours for stabilization. The temperature of Ringer's solution was kept at 37 ± 1˚C as this is the normal temperature of the human body. The temperature was maintained using a heating mantle. The exposed area of the samples in the Ringer's solution was 1.92 cm^2. The 316L SS specimen forms the working electrode. All potentials were measured with respect to a saturated calomel electrode as the reference electrode. A graphite rod served as the counter electrode. All the tests were performed at a scan rate of 1 mV/sec and fresh solution was used for each experiment. The corrosion rate was determined using the Tafel plots sweeping potential from-250 mV to +250 mV relative to open circuit potential and all the tests were carried out on several samples as at least three similar results were required to ensure reproducibility.

Results and Discussions

XRD Analysis

The XRD analysis of flame-sprayed HAp coating on AISI 316L SS substrate is shown in Fig. 1. In this figure, tetracalcium phosphate [($Ca_4(PO_4)_2O$), TTCP] is represented by symbol (T) and b-tricalcium phosphate [($Ca_3(PO_4)_2$), β-TCP] is represented by (β) and HAp by unmarked peaks. The phase composition of as-sprayed HAp coating confirmed the presence of HAp with minor peaks for tetracalcium phosphate [($Ca_4(PO_4)_2O$), TTCP] and tricalcium phosphate [(β-$Ca_3(PO_4)$].

The peak broadening and low intensity of peaks in XRD pattern symbolize the presence of amorphous phases. The XRD analysis of flame-sprayed HAp/TiO_2 coating on 316L SS substrate is shown in Fig.2. In this figure, tetracalcium phosphate [($Ca_4(PO_4)_2O$), TTCP] is represented by symbol (T) and b-tricalcium phosphate [($Ca_3(PO_4)_2$), β-TCP] is represented by (β) and HAp by unmarked peaks. The phase composition of the HAp/ TiO_2 bond coating consists of HAp with minor peaks of β-TCP and TTCP phases. The XRD analysis of the as-sprayed HAp/TiO_2 bond coating indicated the presence of amorphous phase as observed from the broad peaks.

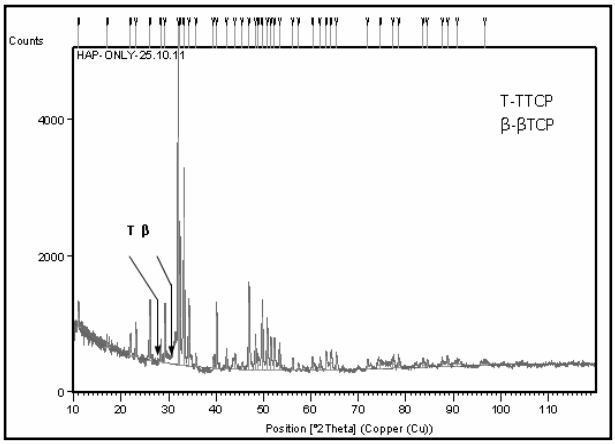

Fig. 1: X-ray Diffraction Pattern of As-sprayed HAp Coating on 316L SS [TTCP, β-TCP and HAp]

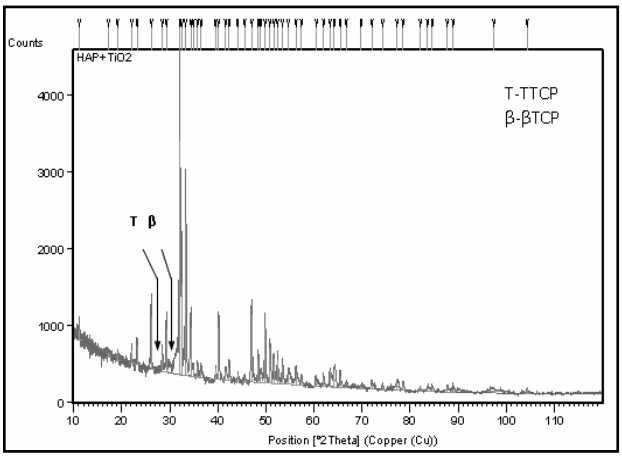

Fig. 2: X-ray Diffraction Pattern of as-sprayed HAp/ TiO_2 Coating on AISI 316L SS [TTCP, β-TCP and HAp]

SEM/ EDS Analysis

SEM micrograph of HAp coating (Fig. 3) shows that the microstructure consists of an uneven microstructure. There is a presence of some small globular particles in the matrix. The EDS point analysis of as-sprayed HAp coating confirmed the presence of significant amounts of Ca, P, and O elements, which are the main elements of HAp. These elements are shown with their atomic percentage data at selected points in Table 2. The Ca/P ratio confirms the presence of different phases in HAp coating. The Ca/P ratio of 1.64 at point 2 in as-sprayed HAp coating is the characteristic of HAp which is very close to theoretical Ca/P ratio of 1.67. The Ca/P ratio of 1.46 and 1.69 at points 1 and 3 indicates the formation of tetracalcium phosphate [$(Ca_4(PO_4)_2O)$, TTCP] phase. The fraction of HAp, TTCP and β-TCP phases present in the HAp coatings determines their in-vivo biological behavior [9].

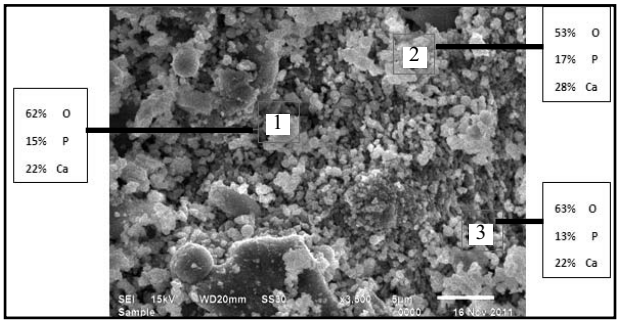

Fig. 3: FE-SEM Analysis along with EDS Point Analysis Showing the Elemental Composition of Flame-sprayed HAp Coating on 316L SS

Table 2: Ca/ P Ratio of Flame Sprayed HAp Coating at Selected Points

HAp Coating	Point 1	Point 2	Point 3
Ca/P Ratio	1.46	1.64	1.69

The HAp/ TiO_2 bond coating (Fig. 4) consists of a small spherical particles densely packed together. The EDS point analysis of HAp/ TiO_2 coated surface confirms the presence of Ca, P, and O elements. There are no indications of Ti on the surface of HAp/ TiO_2 coated specimens. It shows that the bond coating of TiO_2 is completely covered with a HAp top coat.

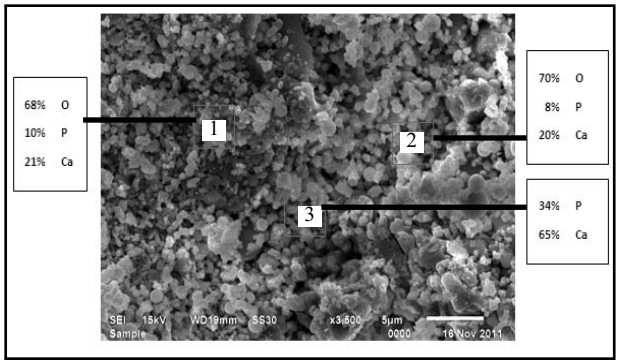

Fig. 4: FE-SEM Analysis along with EDS Point Analysis Showing the Elemental Composition of Flame-sprayed HAp/ TiO_2 Bond Coating on 316L SS

Electrochemical Polarization Behavior

The potentio-dynamic curves of bare and flame-sprayed HAp and HAp/ TiO_2 bond coated 316L SS specimens in Ringer's solution at 37±1˚C temperature are shown in Fig. 5, 6 and 7 respectively.

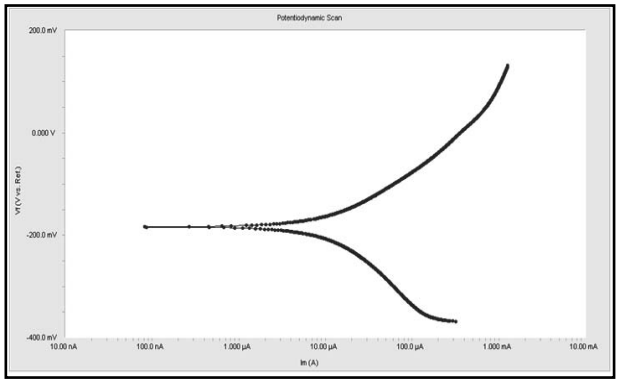

Fig. 5: Potentio-dynamic Curves of Uncoated 316L SS Specimen in Ringer's Solution at 37 ± 1 ˚C

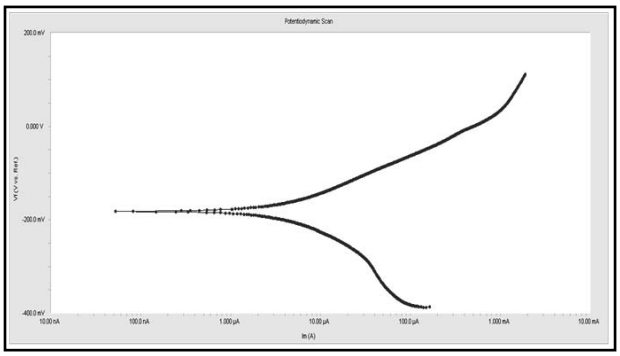

Fig. 6: Potentio-dynamic Curves of Flame-sprayed HAp Coated 316L SS Specimens in Ringers Solution at 37 ± 1˚C

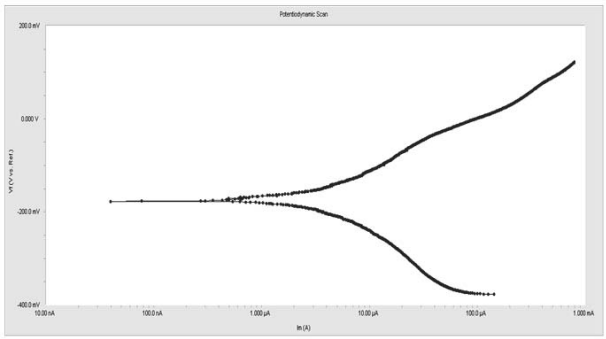

Fig. 7: Potentio-dynamic Curves of Flame-sprayed HAp/ TiO_2 Bond Coated 316L SS Specimens in Ringer's Solution at 37 ± 1˚C

The various corrosion parameters are anodic Tafel slope (β_a), cathodic Tafel slope (β_c), corrosion potential (E_{Corr}) and corrosion current density (I_{Corr}). The higher the corrosion current density (I_{Corr}) at a given potential, more prone is the material to corrode. According to the analysis of Tafel slope values, the results show that corrosion current density of bare 316L SS in Ringer's solution (I_{Corr}= 9.85 μAcm^{-2}, E_{Corr}=-184.0 mV) is higher than the HAp coated samples (I_{Corr}= 5.83 μAcm^{-2}, E_{Corr}=-1.82 mV) and higher than the HAp/TiO_2 bond coated samples (I_{Corr}= 3.66 μAcm^{-2}, E_{Corr}=-1.77 mV). Corrosion parameters determined by the Tafel extrapolation method are summarized in Table 3.

Table 3: Corrosion Parameters Determined by the Tafel Extrapolation Method

Parameters	Uncoated	HAp Coated	HAp/ TiO_2 Coated
β_a (e^{-3} V/decade)	93.1	111.5	148.4
β_c (e^{-3} V/decade)	11.4	136.3	113.9
E_{Corr} (mV)	-184.0	-1.82	-1.77
I_{Corr} (μAcm^{-2})	9.85	5.83	3.66

The polarization curve for the HAp and HAp/TiO_2 coating was shifted to the left when compared to bare 316L SS curve. The lower I_{Corr} values of the HAp and HAp/TiO_2 bond coated specimens indicate that they are more corrosion resistant than bare 316L SS specimens in Ringer's solution. These results are in agreement with previous corrosion studies on HAp coating and HAp/TiO_2 bond coating [10–11].

Conclusion

The following conclusions have been drawn from the present study:

a. The HAp and HAp / TiO_2 coatings were deposited successfully on 316L SS by using CERAJET flame spraying apparatus.

b. Presence of Ca, P and O in the as-sprayed coating was confirmed by the EDS analysis.

c. The electrochemical study showed an improvement in the corrosion resistance of the 316L SS after the deposition of flame-sprayed HAp and HAP/TiO_2 coatings in simulated human body fluid conditions.

Future in-vivo studies of flame-sprayed HAp and HAp/TiO_2 coated 316L SS and further complete interpretation of these results can help in assessing their use in clinical applications.

Acknowledgment

The authors express their sincere thanks to Dr. Harpreet Singh, Assistant Professor, School of Mechanical, Materials and Energy Engineering, Indian Institute of Technology, Roopnagar (Punjab) for his kind co-operation during this research work.

References

[1] Ahmad, A. and Alsaad, A. (2007), "Adhesive B-doped DLC Films on Biomedical alloys Used for Bone Fixation", *Bull. Mater. Sci*., Vol. 30, No. 4, August, Vol. A247, pp. 529–551.

[2] Park. J.B. (2000), *The Biomedical Engineering Handbook*, Vol. 1, J.D. Bronzino, ed., CRC Press LLC, Boca Raton, FL, pp. IV-1-IV-8.

[3] Breme, H.J. and Helsen, J.A. (1998), "Selection of Materials", *Metals as Biomaterials*, John Wiley & Sons Ltd. Baffins Lane, Chichester, England, pp. 1–35.

[4] Kwok, C.T., Wong, P.K, Cheng, F.T. and Man, H.C. (2009), "Characterization and Corrosion Behavior of Hydroxyapatite Coatings on Ti-6Al-4V Fabricated by Electrophoretic Deposition", *Applied Surface Science*, Vol. 255, Issues 13–14, April, pp. 6736–6744.

[5] Qiu, D., Wang, A. and Yin, Y., "Characterization and Corrosion Behavior of Hydroxyapatite/ zirconia Composite Coating on Ni-Ti Fabricated by Electrochemical Deposition", *Applied Surface Science*, Vol. 255, Issues 13–14, April 2009, pp. 1774–1778.

[6] Bai, Y., Neupane, M.P., Parks, Il, Lee, M.H., Bae, T.S., Watari, F. and Uo, M. (2010), "Electrophoretic Deposition of Carbon Nanotubes–hydroxyapatite Nano-composites on Titanium Substrate", *Materials Science and Engineering C*, Vol. 30, Issue 7, Aug, pp. 1043–1049.

[7] Gopi, D., Collins, V., Prakash, Arun and Kavitha, L., (2009) "Evaluation of Hydroxyapatite Coatings on Borate Passivated 316L SS in Ringer's Solution", *Materials Science and Engineering C*, Vol. 29, Issue 3, Aug, pp. 955–958.

[8] Hiromoto, S. and Yamamoto, A. (2009), "High Corrosion Resistance of Magnesium Coated with Hydroxyapatite Directly Synthesized in an Aqueous Solution", *Electrochimica Acta*, Vol. 54, Issue 27, Nov, pp. 7085–7093.

[9] Weng, J., Liu, Q., Wolke, J.G.C. and Groot, K.D. (1997), "The Role of Amorphous Phase in Nucleating Bone-like Apatite on Plasma-Sprayed Hydroxyapatite Coatings in Simulated Body Fluid", *Journal of Materials Science Letters*, Vol. 16, Issue 4, Aug, pp. 335–337.

[10] Yen, S.K., Chiou, S.H, Wu, S.J., Chang, C.C., Lin, S.P. and Lin, C.M. (2006), "Characterization of Electrolytic HA/ZrO_2 Double Layers Coatings on Ti-6Al-4V Implant Alloy", *Materials Science and Engineering C*, Vol. 26, Issue 1, Jan, pp. 65–77.

[11] Fathi, M.H., Salehi, M., Saatchi, A., Mortazavi, V. and Moosavi, S.B., "In-vitro Corrosion Behavior of Bioceramic, Metallic and Bioceramic-metallic Coated Stainless Steel Dental Implants, *Dental Materials*, Vol. 19, Issue 3, May 2003, pp. 188–19.